




Deliverable D7.08

First validation of Leaf Area Index Maps

V 1.0



The research leading to these results has received funding from the European Union's Horizon 2020 Research and Innovation Programme, under Grant Agreement n° 730074

	D7.08 – First validation of Leaf Area Index Maps		
	Date: 7 November 2018	Version: 1.0	Revision: 1
	H2020 GA N° 730074	Page: 3/26	

Document information

Project Number	730074	Acronym	SENSAGRI
Full Title	Sentinels Synergy for Agriculture		
Project URL	http://sensagri.eu		
Project Coordinator	José F. Moreno. IPL – University of Valencia (Spain)		
EU Project Officer	Massimo Ciscato		

Deliverable	Number	D7.08	Title	First validation of Leaf Area Index Maps
Work Package	Number	WP7	Title	Ground Data Collection and Services Validation

Date of Delivery	Contractual	M24	Actual	M24
Status	Version 1.0		Final x	
Type¹	R <input checked="" type="checkbox"/>	DEM <input type="checkbox"/>	DEC <input type="checkbox"/>	OTHER <input type="checkbox"/> ETHICS <input type="checkbox"/>
Dissemination Level²	PU <input checked="" type="checkbox"/>	CO <input type="checkbox"/>	EU-RES <input type="checkbox"/>	EU-CON <input type="checkbox"/> EU-SEC <input type="checkbox"/>

Responsible partner	ITACYL			
Responsible Author	Name	Vanessa Paredes Gómez	E-mail	pargomva@itacyl.es
	Partner	ITACYL	Phone	+34 983 419500 ext.809306
Other authors	Eatidal Amin and Antonio Ruiz-Verdú (UVEG); David A. Nafría (ITACYL), Michele Rinaldi (CREA)			

Abstract (for dissemination)	In the document we report the first validation of the independent Green LAI and Brown LAI retrievals, obtained with the LAI processor developed by UVEG. The retrieval is based on models that were trained and optimized with LAI ground measurements and S2 data using Gaussian processes regression (GPR).
Keywords	LAI green, LAI brown, assessment of LAI, Sentinel-2, Gaussian processes regression

Version Log			
Issue Date	Rev. No.	Author	Change
31 October 2018	0.1	Vanessa Paredes Gómez	First version
2 November 2018	0.2	David A. Nafría	First review
7 November 2018	1.0	Eatidal Amin	Accepted as final version
7 November 2018	1.0	Antonio Ruiz-Verdú	Final revision

¹ R = Document, report; DEM = Demonstrator, pilot, prototype; DEC = Websites, patent fillings, videos, etc; OTHER; ETHICS = Ethics requirement

² PU = Public; CO = Confidential (Consortium and Commission Services); EU-RES = Restreint UE; EU-CON Confidential UE; EU-SEC = Secret UE (Commission Decision 2005/444/EC)

Table of Contents

Document information.....	3
List of Figures.....	5
1. Introduction.....	7
1.1. Scope of the document	7
1.2. Notations, abbreviations and acronyms	7
2. Performance measures	8
3. Leaf Area Index Products.....	9
4. Validation in the core European test sites	9
4.1. Spanish test site: 2017-2018	9
4.1.1. Reference data	9
4.1.2. Green LAI evaluation	12
4.1.3. Brown LAI evaluation	14
4.2. Italian test site: 2017	16
4.2.1. Reference data	16
4.2.2. Green LAI evaluation	16
4.2.3. Brown LAI evaluation	17
4.3. Polish test site: 2017	19
4.3.1. Reference data	19
4.3.2. Green LAI evaluation	19
4.4. Joint assessment (all test sites together)	21
4.4.1. Green LAI	21
4.4.2. Brown LAI	23
5. Conclusions.....	24
5.1. General validation results	24
5.2. Product suitability	25
Reference documents	26
Web references	26

List of Figures

Figure 1. Comparison of Green LAI values obtained with LICOR-LAI and ACCUPAR and out layer detection. Blue line = 1:1 line; pink line = linear fit; Green line = tolerance limit.....	10
Figure 2. Comparison of Green LAI values obtained with LICOR-LAI and ACCUPAR after eliminating the outliers values. Blue line = 1:1 line; pink line = linear fit; Green line = tolerance limit.....	10
Figure 3. Comparison of Brown LAI values obtained with LICOR-LAI and ACCUPAR and out layer detection. Blue line = 1:1 line; pink line = linear fit; Green line = tolerance limit.....	11
Figure 4. Comparison of Brown LAI values obtained with LICOR-LAI and ACCUPAR after eliminating the outliers values. Blue line = 1:1 line; pink line = linear fit; Green line = tolerance limit.....	11
Figure 5. Scatter plot of the Green LAI index with the estimated SENSAGRI LAI versus the LAI ground data measured by LICOR-LAI.	12
Figure 6. Scatter plot of the Green LAI index with the estimated SENSAGRI LAI versus the LAI ground data measured by LICOR-LAI. The SENASGRI LAI data with a CV above 40% were filtered out.....	12
Figure 7. Scatter plot of the Green LAI index with the estimated SENSAGRI LAI versus the LAI ground data measured by ACCUPAR.	13
Figure 8. Scatter plot of the Green LAI index with the estimated SENSAGRI LAI versus the LAI ground data measured by ACCUPAR. The LAIG data with a CV above 40% were filtered out.....	13
Figure 9. Coefficient of variation for Green LAI values retrieved by GPR model plotted against the values taken by this index in Spanish test site.	13
Figure 10. Scatter plot of the Brown LAI index with the estimated SENSAGRI LAI versus the LAI ground data measured by LICOR-LAI.	14
Figure 11. Scatter plot of the Brown LAI index with the estimated SENSAGRI LAI versus the LAI ground data measured by LICOR-LAI. The LAIB data with a CV above 40% were filtered out.....	14
Figure 12. Scatter plot of the Brown LAI index with the estimated SENSAGRI LAI versus the LAI ground data measured by ACCUPAR.	15
Figure 13. Scatter plot of the Brown LAI index with the estimated SENSAGRI LAI versus the LAI ground data measured by ACCUPAR. The LAIB data with a CV above 40% were filtered out.....	15
Figure 14. Coefficient of variation for Brown LAI values retrieved by GPR model varies according to the values taken by this index in Spanish test site.	15
Figure 15.....	16
Figure 16. Scatter plot of the Green LAI index with the estimated SENSAGRI LAI versus the LAI ground data measured by LICOR-LAI. The LAIG data with a CV above 40% were filtered out	16
Figure 17. Coefficient of variation for Green LAI values retrieved by GPR model plotted against the values taken by this index in Italian test site.....	17
Figure 18. Scatter plot of the Brown LAI index with the estimated SENSAGRI LAI versus the LAI ground data measured by LICOR-LAI.	18
Figure 19. Scatter plot of the Brown LAI index with the estimated SENSAGRI LAI versus the LAI ground data measured by LICOR-LAI. The LAIB data with a CV above 60% were filtered out.....	18
Figure 20. Coefficient of variation for Brown LAI values retrieved by GPR model varies according to the values taken by this index in Italian test site.....	18
Figure 21. Scatter plot of the Green LAI index with the estimated SENSAGRI LAI versus the LAI ground data measured by LICOR-LAI.	19
Figure 22. Scatter plot of the Green LAI index with the estimated SENSAGRI LAI versus the LAI ground data measured by LICOR-LAI. The LAIG data with a CV above 40% were filtered out.	19
Figure 23. Coefficient of variation for Green LAI values retrieved by GPR model varies according to the values taken by this index in Polish test site.	20

Figure 24. Scatter plot of the Green LAI index with the estimated SENSAGRI LAI versus the LAI ground data measured by LICOR-LAI considering all test site data..... 21


Figure 25. Scatter plot of the Green LAI index with the estimated SENSAGRI LAI versus the LAI ground data measured by LICOR-LAI considering all test site data. The LAIG data with a CV above 40% were filtered out..... 21

Figure 26. Coefficient of variation for Green LAI values retrieved by GPR model plotted against the values taken by this index in all test site together..... 22

Figure 27. Box and whisker plots showing the range values reached by LAI ground data and LAI estimates for durum wheat in March in the same location: Italian test site..... 22

Figure 28. Scatter plots of the Brown LAI index with the estimated SENSAGRI LAI versus the LAI ground data measured by LICOR-LAI considering all test site data and employing different thresholds to filter data based on the coefficient of variation of the LAIB estimates..... 23

Figure 29. Coefficient of variation for Brown LAI values retrieved by GPR model plotted against the values taken by this index in all test site together..... 23

	D7.08 – First validation of Leaf Area Index Maps		
	Date: 7 November 2018	Version: 1.0	Revision: 1
	H2020 GA N° 730074	Page: 7/26	


1. Introduction

1.1. Scope of the document

The present document provides the main results of the first validation of the SENSAGRI Green LAI and Brown LAI products, both derived independently with the LAI processor developed by UVEG. The retrieval is based on models that were trained and optimized with LAI ground measurements and S2 data using Gaussian processes regression (GPR).

1.2. Notations, abbreviations and acronyms

ARTMO	Automated Radiative Transfer Models Operator
CV	Coefficient of Variation
GPR	Gaussian Processes Regression
LAI	Leaf Area Index
LAIG	Green Leaf Area Index
LAIB	Brown Leaf Area Index (only when the crop is senescent)
NRMSE	Normalized Root-mean-squared error
R2	Coefficient of determination
S2	Sentinel-2
SD	Standard deviation

	D7.08 – First validation of Leaf Area Index Maps		
	Date: 7 November 2018	Version: 1.0	Revision: 1
	H2020 GA N° 730074	Page: 8/26	

2. Performance measures

The performance of the product has to be evaluated to assess the uncertainty of calibrated Sentinel1/2 LAI estimates. The uncertainty metrics calculated are those described by Sexton et al., 2013, based on root mean squared error (RMSE):

$$RMSE = \sqrt{\frac{\sum_{i=1}^n (M_i - R_i)^2}{n}}$$

where M_i and R_i are estimated and reference LAI values at an ESU i in a set of n units, randomly selected among the whole data set of ESUs selected for validation, so to be representative of the LAI variation per each type of crop grown in the study area. After modelling the relationship between M_i and R_i by linear regression, RMSE can be split into components: systematic error (MSE_S) and unsystematic error (MSE_U):


$$MSE_S = \sum_{i=1}^n \frac{(\hat{M}_i - R_i)^2}{n}$$

$$MSE_U = \sum_{i=1}^n \frac{(M_i - \hat{M}_i)^2}{n}$$

where \hat{M}_i is the LAI value predicted by the linear relationship (Willmott, 1982). Accuracy is quantified by the difference between the trend of the model over reference LAI (MSE_S), whereas precision by the variation around this trend (MSE_U). As MSE_S and MSE_U sum to Mean-Square Error (MSE), it results:

$$RMSE = \sqrt{MSE_S + MSE_U}$$

For consistency, all the errors should be expressed in terms of root mean squared errors.

	D7.08 – First validation of Leaf Area Index Maps		
	Date: 7 November 2018	Version: 1.0	Revision: 1
	H2020 GA N° 730074	Page: 9/26	

3. Leaf Area Index Products

Leaf Area index maps are stored in multiband GEOTIFF files. Each file contains 8 bands (Green LAI index, Brown LAI index, Total LAI and precision parameters) The files are produced according to SENSAGRI proposed algorithm with software version 0.20. The spatial resolution is 20m, the Spatial reference system is WGS84 in UTM projection (site-specific UTM zone).

Together with the tiff file, there is a text file with some metadata information. There are some metadata info in the file name according to Deliverable D4.04.

Note that only the bands with Green LAI index or Brown LAI index data have been validated. The band of coefficient variation has been used as a source of relative uncertainty in order to filter out likely inaccurate data.

4. Validation in the core European test sites

The validation presented here consists of comparing the Elementary Sample Units (ESU) LAI measurement against the SENSAGRI LAI product pixel value, corresponding to the centre coordinates of the sampled ESU. Thus, five LAI measurements were collected in each ESU, according the Fig. 1 of the D7.03. (Sampling approach for each ESU). The individual LAI field measurements were done at ESU level using a non-destructive method with the LAI-2000 Plant Canopy Analyser (hereinafter LICOR-LAI) and the ceptometer ACCUPAR model LP-80 (hereinafter ACCUPAR). The smallest extent of elementary sampling unit (ESU) is defined as the minimum area compatible with the resolution of the satellite product to be validated. The objective of the sampling strategy is to use the pattern of ESUs, to capture the variability across the site extent, and the repeated measurements within the each ESU, to capture the variability within the high spatial resolution imagery (~20 m). Thus, five LAI measurements were collected in each ESU, according the Fig. 1 of the D7.03. (Sampling approach for each ESU).

As mentioned before, only the bands with Green LAI index or Brown LAI index data have been validated. However, the band with coefficient variation has been used as a source of relative uncertainty in order to filter out inaccurate data and refine the validation dataset. In particular, the coefficient of variation for each SENSAGRI LAI product, retrieved by the GPR model, has been plotted against the values taken by the index itself in order to find a threshold to use in filtering data.

This validation is split in two parts: Green LAI and Brown LAI. The field data comes from Spain, Italy and Poland. These datasets were the only ones available at the time of writing this report. Note that more LAI ground data were collected besides but those were used to train the LAI algorithm.

4.1. Spanish test site: 2017-2018

4.1.1. Reference data

For the Spanish test site, there are two distinct sets of validation data for **Green LAI**: the first one is a series of campaigns done only with ACCUPAR LP-80 (85 ESUs between 2017 and 2018), and the second one is a series of campaigns using both instruments, LICOR-LAI and ACCUPAR, simultaneously (23 ESUs

in total, 11 in June 2017 and 12 in July 2018). So, these LICOR-LAI+ACCUPAR validation dataset comprises field campaigns from 2017 and 2018 where main crops measured for green LAI index were sunflower, sugar beet, potato, maize and alfalfa. For **Brown LAI** the main crops observed were straw cereals and rapeseed. For this report, only data coming for LICOR-LAI+ACCUPAR group is used.

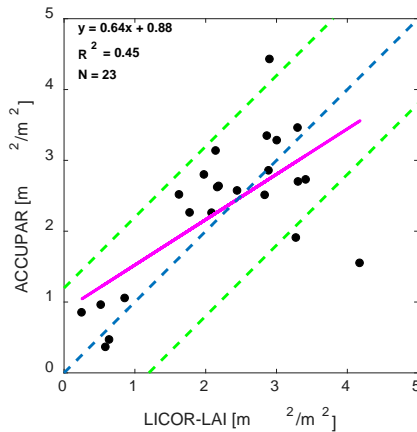


Figure 1. Comparison of Green LAI values obtained with LICOR-LAI and ACCUPAR and out layer detection. Blue line = 1:1 line; pink line = linear fit; Green line = tolerance limit.

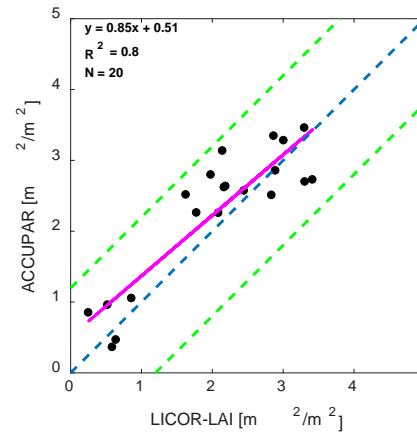


Figure 2. Comparison of Green LAI values obtained with LICOR-LAI and ACCUPAR after eliminating the outliers values. Blue line = 1:1 line; pink line = linear fit; Green line = tolerance limit.

Some remarkable discrepancies can be observed between measurements carried out with different instruments. In order to select the more reliable ESUs for the validation process, Green LAI points with values above or below the lines equal to of the absolute mean error of the differences of all LICOR-LAI - ACCUPAR points plus or minus one standard deviation of the data differences (± 1.19) respect the 1:1 line have been discarded. These points are considered unreliable ground points and are not used for doing the validation. Figure 2 represents the final dataset used for validation based on 20 ESUs after filtering 3 ESUs.

Regarding Brown LAI, 31 ESUs were collected in a campaign in July 2018. Figures 3 and 4 show the scatter plot with LAI ground data using both instruments (LICOR-LAI and ACCUPAR), and also, how to filter the outliers out using the same procedure as for the Green LAI, as explained above. In this case, the green lines representing the tolerance interval setting by means of the absolute mean error of the differences of all LICOR-LAI - ACCUPAR points plus or minus one standard deviation of the data differences (± 0.9), respect the 1:1 line. Outside this threshold, the measures can be considered unreliable ground points and therefore, they are not including in the validation dataset. Figure 4 represents the final dataset used for validation based on 25 ESUs.

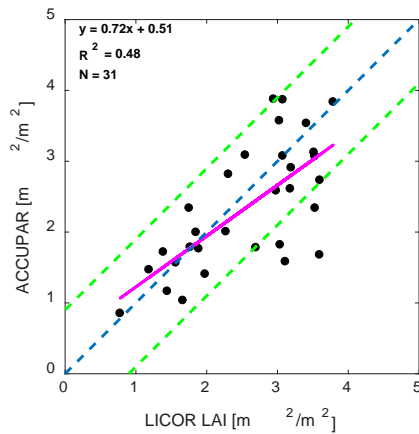


Figure 3. Comparison of Brown LAI values obtained with LICOR-LAI and ACCUPAR and out layer detection. Blue line = 1:1 line; pink line = linear fit; Green line = tolerance limit.

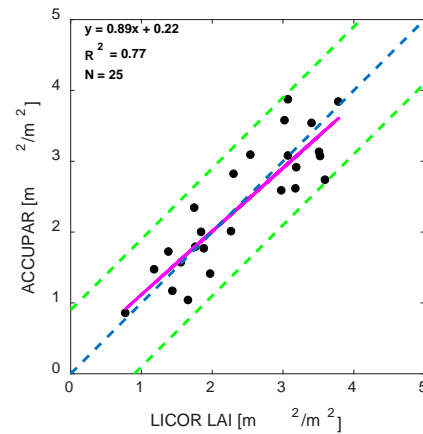


Figure 4. Comparison of Brown LAI values obtained with LICOR-LAI and ACCUPAR after eliminating the outliers values. Blue line = 1:1 line; pink line = linear fit; Green line = tolerance limit.

In this test site, validation graphs and statistics were calculated comparing LAI ground measurements from both instruments and the SENSAGRI Green/Brown LAI products.

4.1.2. Green LAI evaluation

Figure 5 and Figure 6 show the validation results without applying and applying an uncertainty threshold using the coefficient of variation of the LAI estimates by the GPR model, respectively. Error bars represent the standard deviation of the LAI measured with the LICOR-LAI (x axis) and the intrinsic standard deviation provided by the GPR retrieval model (y axis). There is a lack of information about standard deviation of LICOR-LAI ground data for the 2017 field campaign.

Applying the uncertainty threshold (CV= 0-40%, same criteria used in the maps) contributes to increase the associated error and leads to worse correlation statistics.

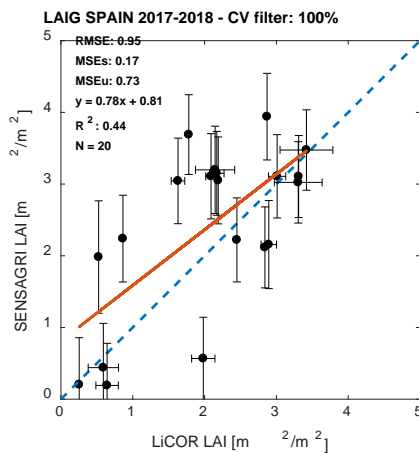


Figure 5. Scatter plot of the Green LAI index with the estimated SENSAGRI LAI versus the LAI ground data measured by LICOR-LAI.

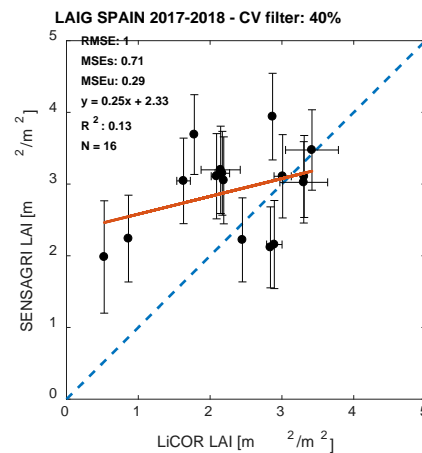


Figure 6. Scatter plot of the Green LAI index with the estimated SENSAGRI LAI versus the LAI ground data measured by LICOR-LAI. The SENSAGRI LAI data with a CV above 40% were filtered out.

In the same way as before, figure 7 and figure 8 show the validation results applying two different thresholds for the CV filter. Error bars represent the standard deviation of the LAI measured with the ACCUPAR instrument (x axis) and the intrinsic standard deviation provided by the GPR retrieval model (y axis). In this case, when removing the points whose CV is higher than 40% (Figure 8), the error decreases, although a worse correlation is obtained. In this case, the same analysis performed with ACCUPAR, shows better results to the ones obtained with LICOR-LAI instrument.

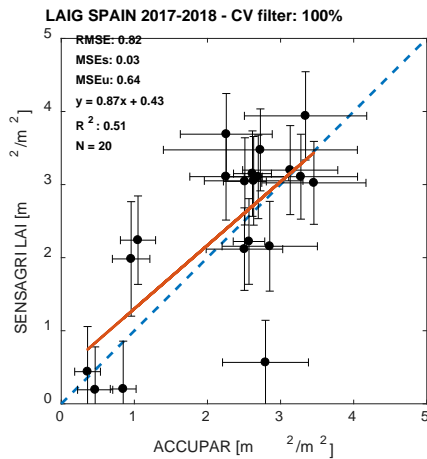


Figure 7. Scatter plot of the Green LAI index with the estimated SENSAGRI LAI versus the LAI ground data measured by ACCUPAR.

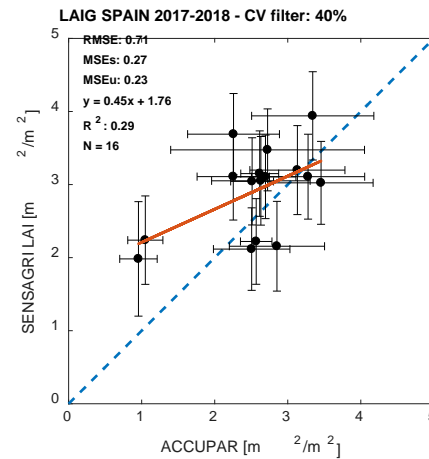


Figure 8. Scatter plot of the Green LAI index with the estimated SENSAGRI LAI versus the LAI ground data measured by ACCUPAR. The LAIG data with a CV above 40% were filtered out.

Figure 9 represents the model uncertainty of the retrieved Green LAI values retrieved by the GPR model (hereinafter LAIG values) for the Spanish validation dataset. This figure shows how the intrinsic coefficient of variation, provided as an output of the GPR, decreases as LAIG values increase, following a negative exponential curve. It is important to highlight that this so-called “intrinsic” CV represents the uncertainty derived from the training of the model and is different from the estimate that could be done later from validation data. In any case, it indicates that the model predicts a higher error towards lower LAIG estimates.

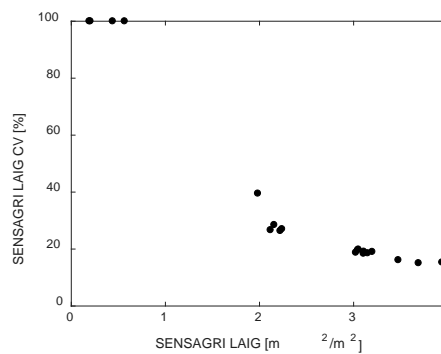


Figure 9. Coefficient of variation for Green LAI values retrieved by GPR model plotted against the values taken by this index in Spanish test site.

4.1.3. Brown LAI evaluation

Figure 10 and Figure 11 show the validation results without applying and applying an uncertainty threshold (filtering according to the CV value), respectively. Error bars represent the standard deviation of the LAI measured with the LICOR-LAI (x axis) and the standard deviation provided by the GPR retrieval model (y axis). One point was removed from the training database because the GPR model threw an exception, as a negative value was retrieved, which cannot be possible for a biophysical parameter. Therefore, in total 24 LAI points are used for the validation.

Applying the uncertainty threshold to include only those LAI pair of points whose associated CV value is within the threshold ($CV < 40\%$) helps reduce all the errors (RMSE, MSE_s , MSE_u), but does not improve neither the linear fitting nor the R^2 .

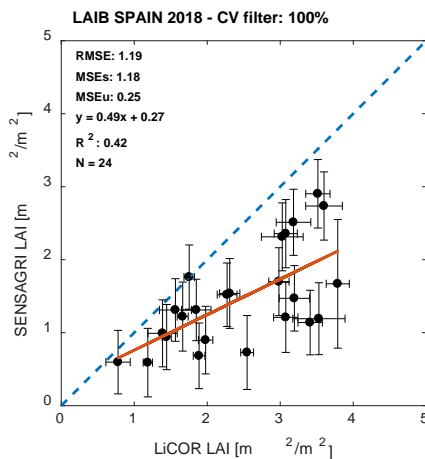


Figure 10. Scatter plot of the Brown LAI index with the estimated SENSAGRI LAI versus the LAI ground data measured by LICOR-LAI.

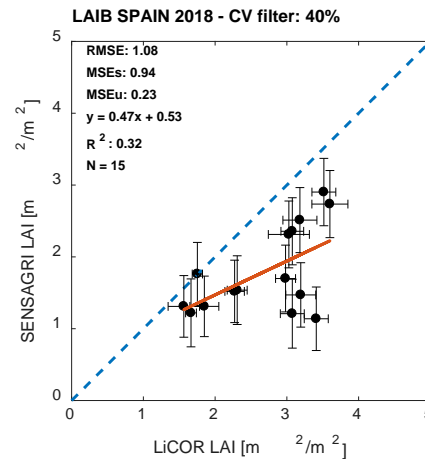


Figure 11. Scatter plot of the Brown LAI index with the estimated SENSAGRI LAI versus the LAI ground data measured by LICOR-LAI. The LAIB data with a CV above 40% were filtered out.

Figure 12 and Figure 13 show the validation results without applying and applying the CV filter, respectively. Error bars represent the standard deviation of the LAI measured with the ACCUPAR instrument (x axis) and the (“intrinsic”) standard deviation provided by the GPR retrieval model (y axis). In this case, when removing the points whose CV is higher than 40% (Figure 13), the error decreases, although a worse correlation is obtained.

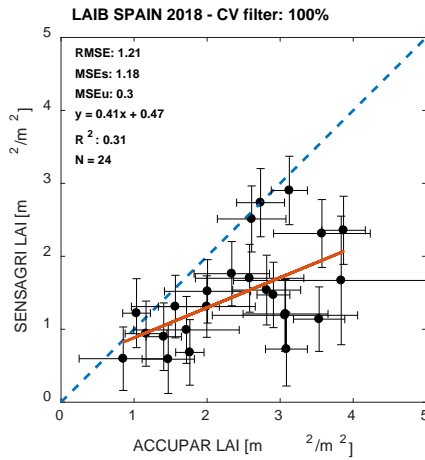


Figure 12. Scatter plot of the Brown LAI index with the estimated SENSAGRI LAI versus the LAI ground data measured by ACCUPAR.

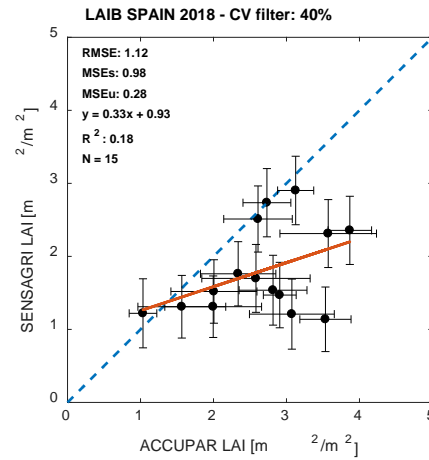


Figure 13. Scatter plot of the Brown LAI index with the estimated SENSAGRI LAI versus the LAI ground data measured by ACCUPAR. The LAIB data with a CV above 40% were filtered out.

Figure 14 represents the model uncertainty of the retrieved Brown LAI values for the validation data.

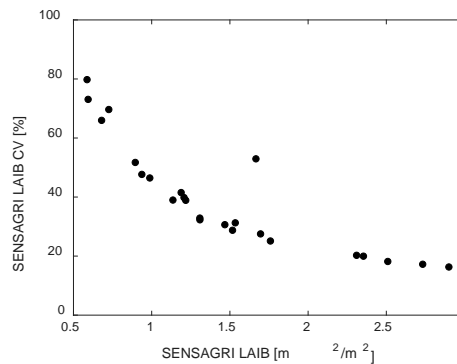


Figure 14. Coefficient of variation for Brown LAI values retrieved by GPR model varies according to the values taken by this index in Spanish test site.

4.2. Italian test site: 2017

4.2.1. Reference data

A total of 76 ESUs were measured to obtain Green LAI index following the procedure by means of LICOR-LAI instrument in several field campaigns from March to June 2017. Main crops are durum wheat, barley, tomato and chickpeas. There is no other instrument used so all data without filtering is used in the validation

Regarding Brown LAI, 16 ESUs were collected over senescent durum wheat during May 2017. The range of the measurements was not wide and the LAI values ranged from 1 to 2.4.

4.2.2. Green LAI evaluation

The validation results are shown in the figures below without applying (Figure 15) and applying (Figure 16) an uncertainty threshold using the coefficient of variation of the LAI estimates by the GPR model, respectively. Error bars represent the standard deviation of the LAI measured with the LICOR-LAI (x axis) and the standard deviation provided by the GPR retrieval model (y axis).

Applying the uncertainty threshold (CV= 0-40%, same criteria used in the maps) contributes to increase the RMSE and leads to worse correlation statistics.

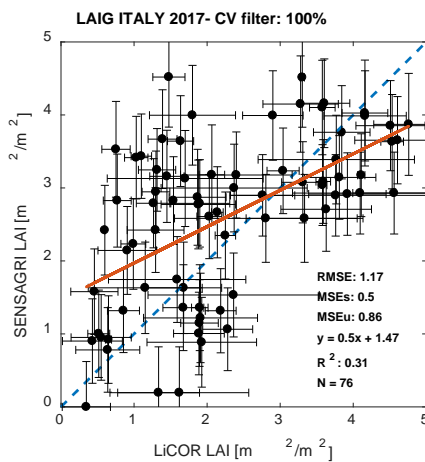


Figure 15. Scatter plot of the Green LAI index with the estimated SENSAGRI LAI versus the LAI ground data measured by LICOR-LAI.

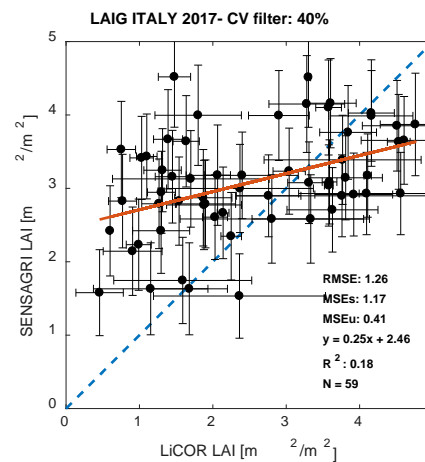


Figure 16. Scatter plot of the Green LAI index with the estimated SENSAGRI LAI versus the LAI ground data measured by LICOR-LAI. The LAIG data with a CV above 40% were filtered out

Figure 17 represents the model uncertainty of the retrieved LAIG values for the Italian validation dataset. This figure shows how the coefficient of variation decreases as LAIG values increase, following a negative exponential curve. In particular, a high uncertainty exists in LAIG values below one with a CV associated around 40%. From this value, the uncertainty gradually increases.

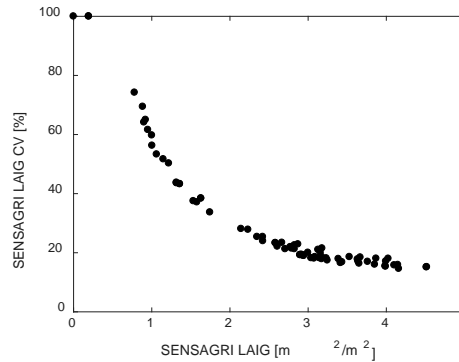


Figure 17. Coefficient of variation for Green LAI values retrieved by GPR model plotted against the values taken by this index in Italian test site.

4.2.3. Brown LAI evaluation

For the Italian test site, the validation data consists of 17 ESUs of wheat crop sampled in May 2017 using the LICOR-LAI instrument. Due to a negative model retrieval, one LAI point was removed from the validation dataset. In this case, the model uncertainty was relatively high for all the LAIB retrieved points. If applying a CV filter of 40 % all points would be masked out. Figure 19 shows the LAIB results within an uncertainty threshold of 60%. In this case and contrary to Spanish case, applying this filter of CV 60% it helps reduce all the errors (RMSE, MSE_s, MSE_u), improve the linear fitting and the correlation coefficient (R²). However, the data deletion is so high that it seems to be necessary to make a more exhaustive control of all the available data.

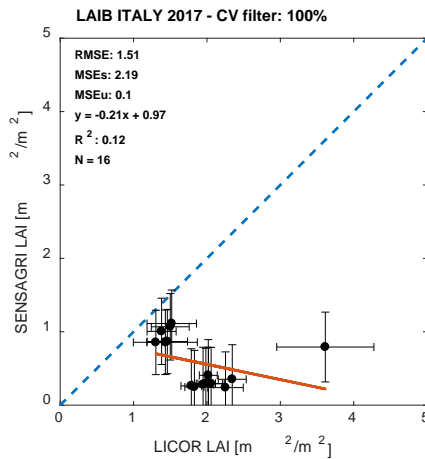


Figure 18. Scatter plot of the Brown LAI index with the estimated SENSAGRI LAI versus the LAI ground data measured by LICOR-LAI.

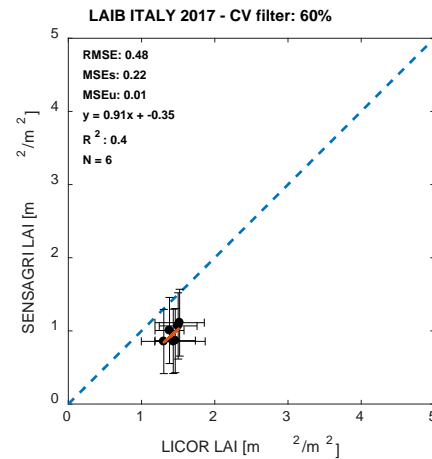


Figure 19. Scatter plot of the Brown LAI index with the estimated SENSAGRI LAI versus the LAI ground data measured by LICOR-LAI. The LAIB data with a CV above 60% were filtered out.

Figure 20 represents the model uncertainty of the retrieved LAIB values for the validation data. This figure shows how the coefficient of variation decreases as LAIG values increase, following a negative exponential curve. In particular, a high uncertainty exists in LAIG values below 0.8 with a CV associated around 60%. From this value, the uncertainty is dramatically increased

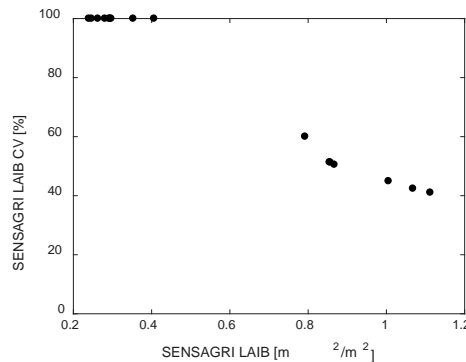


Figure 20. Coefficient of variation for Brown LAI values retrieved by GPR model varies according to the values taken by this index in Italian test site.

4.3. Polish test site: 2017

4.3.1. Reference data

In this test site, only Green LAI data is available. The campaigns took place in April-May-June 2017. Main sampled crops are maize, winter wheat, oil seed rape. There is a total of 26 ESUs measured with LAI-2000 instrument (LICOR-LAI). In this dataset, there is a lack of standard deviation information.

4.3.2. Green LAI evaluation

The validation results are shown in the figures below without applying (Figure 15) and applying (Figure 16) an uncertainty threshold using the coefficient of variation of the LAI estimates by the GPR model, respectively. Error bars represent the standard deviation of the LAI measured with the LICOR-LAI (x axis) and the standard deviation provided by the GPR retrieval model (y axis).

Applying the uncertainty threshold (CV= 0-40%, same criteria used in the maps) contributes to increase the RMSE and leads to worse correlation statistics

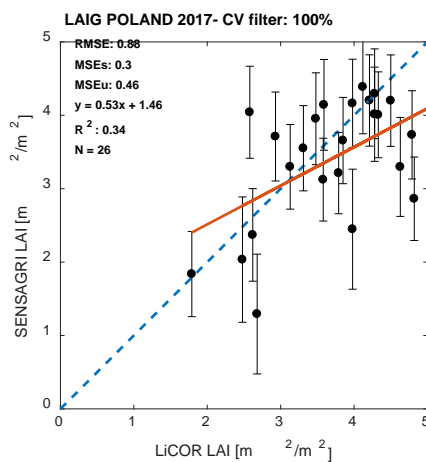


Figure 21. Scatter plot of the Green LAI index with the estimated SENSAGRI LAI versus the LAI ground data measured by LICOR-LAI.

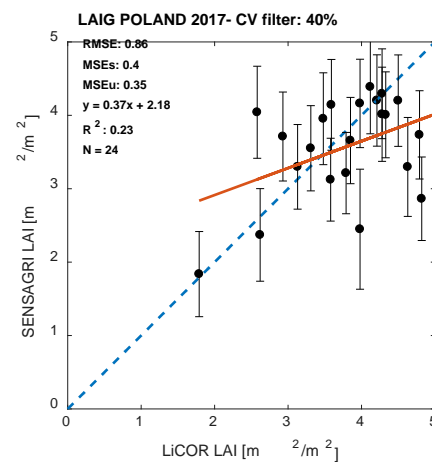


Figure 22. Scatter plot of the Green LAI index with the estimated SENSAGRI LAI versus the LAI ground data measured by LICOR-LAI. The LAIG data with a CV above 40% were filtered out.

Figure 23 represents the model uncertainty of the retrieved LAIG values for the validation dataset.

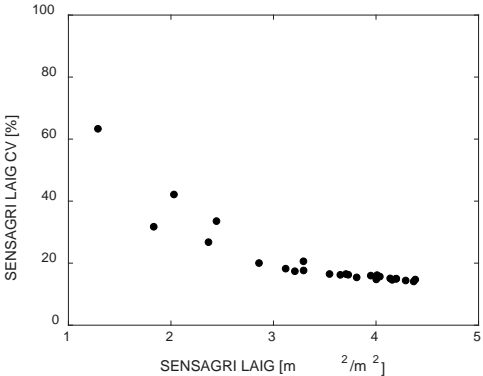


Figure 23. Coefficient of variation for Green LAI values retrieved by GPR model varies according to the values taken by this index in Polish test site.

4.4. Joint assessment (all test sites together)

4.4.1. Green LAI

Finally, the figure 24 shows the validation results for Green LAI considering all the SENSAGRI test sites validation datasets together. The figure 25 shows the same data except those discarded employing a threshold for filtering outliers by coefficient of variation above 40%.

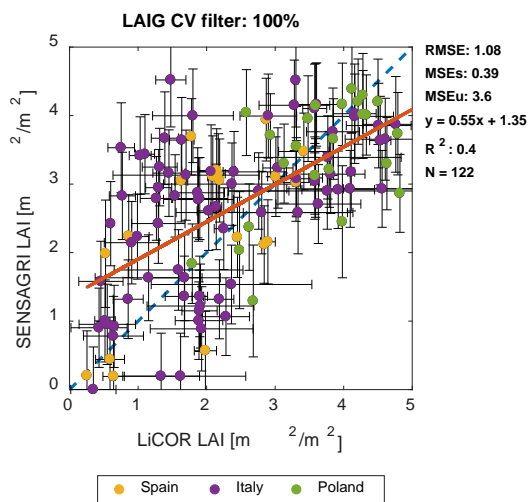


Figure 24. Scatter plot of the Green LAI index with the estimated SENSAGRI LAI versus the LAI ground data measured by LICOR-LAI considering all test site data.

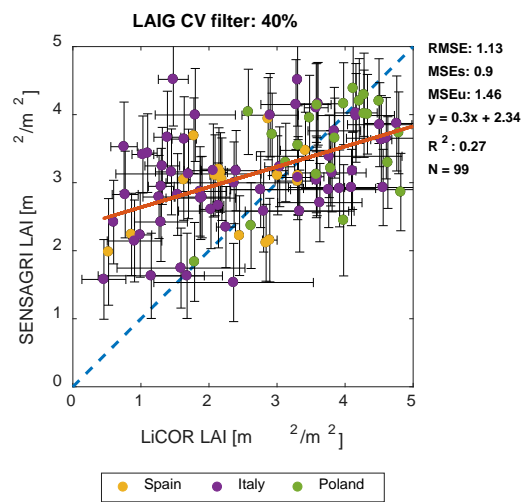


Figure 25. Scatter plot of the Green LAI index with the estimated SENSAGRI LAI versus the LAI ground data measured by LICOR-LAI considering all test site data. The LAIG data with a CV above 40% were filtered out.

Figure 26 represents the model uncertainty of the retrieved LAIG values for all validation dataset together. This figure shows how the coefficient of variation decreases sharply as LAIG values increase, following a negative exponential curve. In particular, for LAIG values below one, the uncertainty gradually increases.

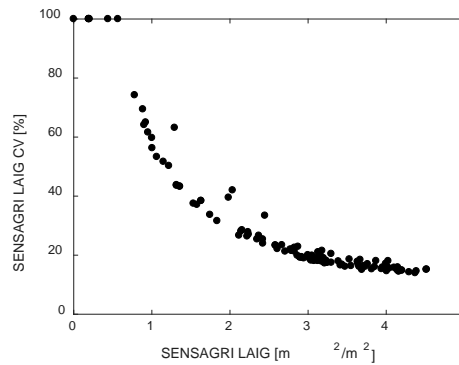


Figure 26. Coefficient of variation for Green LAI values retrieved by GPR model plotted against the values taken by this index in all test site together.

An issue that can be highlighted looking at the figures 24 and 25 is that the LAI ground data behaves in different ways depending on the test site. Particular attention should be given to the validation dataset for Green LAI coming from Italian test site. In this case, there is some doubts about its quality when a very wide range of values is found in the original database considering the same month and the same crop. E.g. values for durum wheat in 14 days of March ranges from 0.43 to 6.97 (See figure 27).

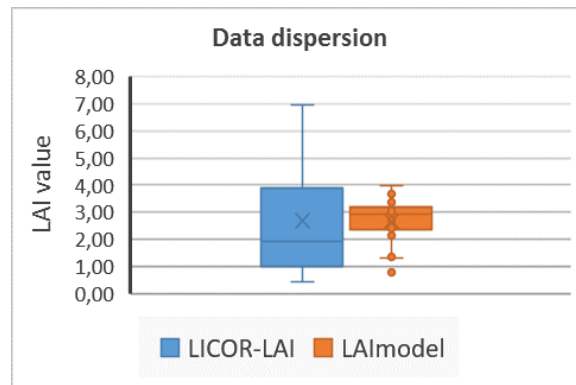


Figure 27. Box and whisker plots showing the range values reached by LAI ground data and LAI estimates for durum wheat in March in the same location: Italian test site.

4.4.2. Brown LAI

Regarding Brown LAI, Figure 28 shows the validation results for this index using all the SENSAGRI test sites validation datasets together and employing a different threshold for filtering outliers by coefficient of variation.

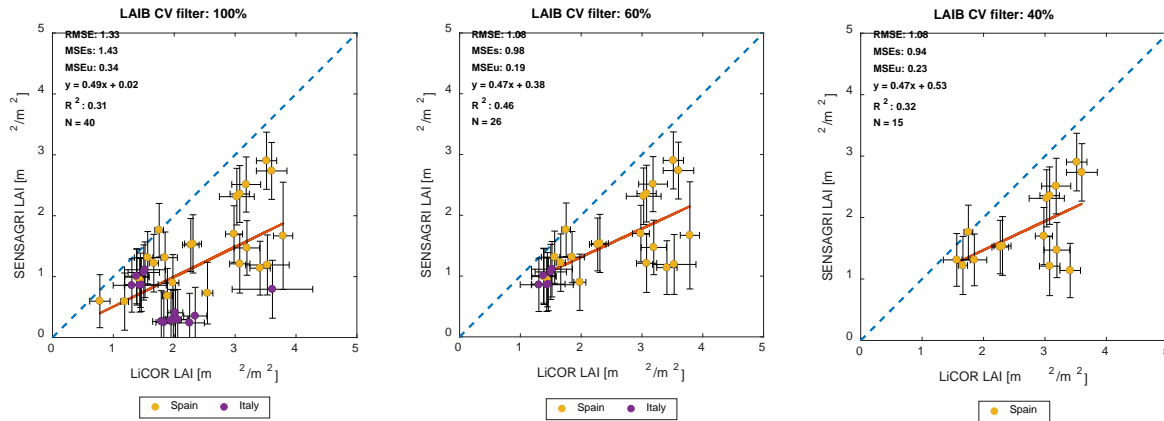


Figure 28. Scatter plots of the Brown LAI index with the estimated SENSAGRI LAI versus the LAI ground data measured by LICOR-LAI considering all test site data and employing different thresholds to filter data based on the coefficient of variation of the LAIB estimates.

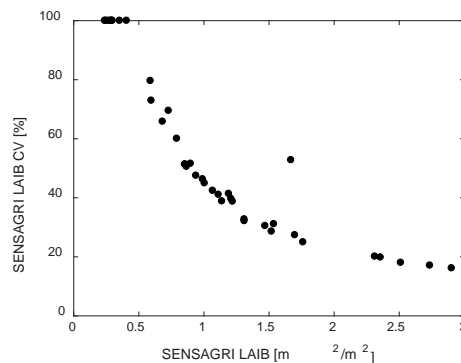



Figure 29. Coefficient of variation for Brown LAI values retrieved by GPR model plotted against the values taken by this index in all test site together.

	D7.08 – First validation of Leaf Area Index Maps		
	Date: 7 November 2018	Version: 1.0	Revision: 1
	H2020 GA N° 730074	Page: 24/26	

5. Conclusions

5.1. General validation results

A first consideration is related to the significance of the uncertainty values (standard deviation and coefficient of variation) provided by the model (called “intrinsic” uncertainty throughout the text). These estimates are currently used for masking out pixels above a certain threshold in the LAI maps. The figures 26 and 29 show that the intrinsic model CV is mainly dependent on the retrieved LAI value. When a threshold of $CV > 40\%$ is set, basically most retrieved values below 1.5 (for LAIG) or 1 (for LAIB) are masked out in the maps. However, for LAIG, those masked pixels are not necessarily producing less accurate results, as shown in figures 24 and 25. For LAIB the results are similar. In fact, figure 28 show that the error statistics for LAIB are almost the same regardless the CV threshold used. Therefore, it can be concluded that the uncertainty provided by the model is not a good indicator of the actual uncertainty of the LAIG and LAIB retrievals.


The uncertainty provided by the model seems to be very dependent on the amount and quality of the field data used for training the Gaussian Processes Regression (GPR). The high uncertainty for low LAI estimates could be related with the high noise and variability of the LAI field measurements for low vegetation coverages, as well as with the fact that there are less low LAI samples in the training dataset. Therefore, the provided CV values could be consider as indicators of the model precision, rather than the model accuracy. They could be kept in the output maps, instead of being filtered out.

The LAIG retrievals show a saturation effect for LAI values greater than 3. In view of the results, the LAIG optimum retrieval range is from 1 to 3. On the other hand, the validation analysis revealed some differences between instruments. Best validation results were obtained in Spain and with the ACCUPAR dataset.

For the LAIB model, there is a systematic underestimation of LAI. In Spain, validation results obtained for LICOR-LAI show less error and better correlation than the ones obtained for the ACCUPAR instrument. A possible reason is that most points of the training database were measured using LICOR-LAI. Particularly for the Spanish validation dataset, the GPR model seems not to be able to retrieve LAIB values higher than 3. On the other hand, LAI values lower than 0.8 are poorly retrieved. Most likely low values are confused with bare soil. Since all data used for training the LAIB model comes from Spain (Valladolid and Albacete), seems reasonable that the retrieval model would perform better in Spain than in Italy. It should be noted that the LAIB GPR model is trained with not a very large number of points, so we cannot expect it to be so robust.

Regarding the error statistics, for LAIG the overall validation (all test sites together) showed that the unsystematic error is higher than the systematic one. On the contrary, for LAIB the systematic component was higher with respect to the unsystematic. This opens the possibility for a correction and further improvement of the accuracy of GPR LAIB by applying calibration factors, whereas for LAIG GPR the improvements could come likely from an improvement on the number and quality of the data of the training dataset.

It should also be reminded that the LAI field measurements, except for the cumbersome destructive methods, tend to be very noisy and rather affected by the instrument used, the illumination conditions, the sampling protocols and the operator interpretation of the measurement procedures. The field experience reveals that for sparse and low canopies the LAI measurements tend to have higher errors. In addition, the time difference between the LAI measurement and the S2 image acquisition introduces


	D7.08 – First validation of Leaf Area Index Maps		
	Date: 7 November 2018	Version: 1.0	Revision: 1
	H2020 GA N° 730074	Page: 25/26	

an added variability to the validation datasets. This affects the overall results of the validation and should be taken into account in its interpretation.

5.2. Product suitability

It would be desirable to provide a metadata file in a standardized format that includes all detailed information about each product provided.

For the next stage of LAI validation, is also recommended to take into account the spatial variability of the LAI model retrievals. In the current validation, the values used were extracted from just pixel per ESU (considering the coordinate center of the ESU). However, a spatial averaging is a more robust approach, if possible incorporating parcel borders' information, to take into account only pixels belonging to the parcels studied in the field.

	D7.08 – First validation of Leaf Area Index Maps		
	Date: 7 November 2018	Version: 1.0	Revision: 1
	H2020 GA N° 730074	Page: 26/26	

Reference documents

- SENSAGRI Deliverable D4.02. Initial operational green & brown LAI prototype. December 26, 2017. Final version
- SENSAGRI Deliverable D4.03. Software of the initial green & brown LAI prototype. Abril, 2018.
- Sexton J.O., Song X.-P., Feng M., Noojipady P., Anand, A., Huang C., Kim D.-H., Collins K.M., Channan S., DiMiceli C., 2013. Global, 30-m resolution continuous fields of tree cover: Landsat-based rescaling of MODIS vegetation continuous fields with lidar-based estimates of error. *Int. J. Digit. Earth* 2013, 6, 427–448.
- Willmott C. J., 1982. Some Comments on the Evaluation of Model Performance. *Bull. Am. Meteorol. Soc.*, 63, 1309–1369.

Web references

- [W1] <http://ipl.uv.es/sensagri/index.php/login>